

Sympathetic Effects of Internal Carotid Nerve Manipulation on Choroidal Vascularity and Related Measures

Juan-Carlos Martinez-Camarillo,^{1,2} Christine K. Spee,³ Michael Chen,⁴ Anthony Rodriguez,³ Kiran Nimmagadda,^{2,5,6} Gloria Paulina Trujillo-Sanchez,^{1,2} David R. Hinton,^{2,3} Alessandra Giarola,⁷ Victor Pikov,⁷ Arun Sridhar,⁷ Mark S. Humayun,^{1,2} and Andrew C. Weitz^{1,2}

¹USC Roski Eye Institute, Keck School of Medicine of the University of Southern California, Los Angeles, California, United States

²USC Ginsburg Institute for Biomedical Therapeutics of the University of Southern California, Los Angeles, California, United States

³Department of Pathology, Keck School of Medicine of the University of Southern California, Los Angeles, California, United States

⁴Department of Biomedical Engineering, Viterbi School of Engineering of the University of Southern California, Los Angeles, California, United States

⁵Neuroscience Graduate Program, University of Southern California, Los Angeles, California, United States

⁶USC - Caltech MD/PhD Program, Los Angeles, California, United States

⁷Galvani Bioelectronics, Stevenage, United Kingdom

Correspondence: Mark S. Humayun, Keck School of Medicine of the University of Southern California, 1450 San Pablo Street, HC4 6545-B, Los Angeles, CA 90033, USA; humayun@med.usc.edu.

Submitted: August 27, 2018

Accepted: September 3, 2019

Citation: Martinez-Camarillo J-C, Spee CK, Chen M, et al. Sympathetic effects of internal carotid nerve manipulation on choroidal vascularity and related measures. *Invest Ophthalmol Vis Sci*. 2019;60:4303–4309. <https://doi.org/10.1167/iovs.18-25613>

PURPOSE. To investigate specific effects of denervation and stimulation of the internal carotid nerve (ICN) on the choroid and retina.

METHODS. Female Sprague Dawley rats underwent unilateral ICN transection ($n = 20$) or acute ICN electrical stimulation ($n = 7$). Rats in the denervation group were euthanized 6 weeks after nerve transection, and eyes were analyzed for changes in choroidal vascularity (via histomorphometry) or angiogenic growth factors and inflammatory markers (via ELISA). Rats in the stimulation group received acute ICN electrical stimulation with a bipolar cuff electrode over a range of stimulus amplitudes, frequencies, and pulse widths. Choroidal blood flow and pupil diameter were monitored before, during, and after stimulation.

RESULTS. Six weeks after unilateral ICN transection, sympathectomized choroids exhibited increased vascularity, defined as the percentage of choroidal surface area occupied by blood vessel lumina. Vascular endothelial growth factor (VEGF) and VEGF receptor-2 (VEGFR-2) protein levels in denervated choroids were 61% and 124% higher than in contralateral choroids, respectively. TNF- α levels in denervated retinas increased by 3.3-fold relative to levels in contralateral retinas. In animals undergoing acute ICN electrical stimulation, mydriasis and reduced choroidal blood flow were observed in the ipsilateral eye. The magnitude of the reduction in blood flow correlated positively with stimulus frequency.

CONCLUSIONS. Modulation of ICN activity reveals a potential role of the ocular sympathetic system in regulating endpoints related to neovascular diseases of the eye.

Keywords: internal carotid nerve, choroidal vascularity, sympathectomy, electrical stimulation

Ocular neovascular diseases, such as exudative (wet) AMD and diabetic retinopathy (DR), are the most common causes of moderate-to-severe vision loss in developed countries.¹ Diseases involving retinal or subretinal neovascularization are accompanied by increased intraocular expression of proangiogenic factors, including different subtypes of vascular endothelial growth factor (VEGF).² Current treatments involve anti-VEGF therapies alone or combined with another medication or laser photocoagulation.^{3,4}

Autonomic innervation of the eye includes sympathetic and parasympathetic pathways via different nerves, including those originating from the superior cervical ganglion (SCG) and pterygopalatine ganglion.⁵ Several lines of evidence suggest a critical role of the sympathetic nervous system in maintaining ocular vascular homeostasis.⁶ The internal carotid nerve (ICN) projects from the SCG to the eye and is the eye's only source of sympathetic innervation.⁷ Prior studies in rat by Steinle et al.^{8,9}

investigated the role of the SCG in regulating choroidal vascularity and related endpoints. These studies reported that surgical removal of the SCG leads to increased choroidal vascularity after 6 weeks. This remodeling is accompanied by photoreceptor cell death arising from apoptosis.¹⁰ A better understanding of autonomic control of the choroid could facilitate development of new therapeutic approaches for ocular neovascular diseases.

Physiologic angiogenesis involves angiogenic and antiangiogenic factors, such as VEGF, pigment epithelium-derived factor (PEDF), and TNF- α . An imbalance in these factors can lead to choroidal neovascularization (CNV), the hallmark pathology of wet AMD. Changes in expression levels of angiogenic growth factors have been reported in rat choroid and retina following SCG removal.^{11–13} In particular, choroidal VEGF and PEDF levels rise following sympathectomy,¹¹ while retinal VEGF and PEDF levels fall.^{12,13} These findings implicate a potential role of

the ocular sympathetic system in CNV, and therefore suggest that the sympathetic nervous system may be involved in wet AMD. Rodent studies have also shown that SCG removal can lead to a DR-like phenotype. Specifically, surgical removal of the SCG in rats causes retinal capillary basement membrane thickening and loss of pericytes after 6 weeks,¹⁴ whereas β -adrenoreceptor (AR)-knockout mice exhibit increased TNF- α protein levels in the retina.^{15,16} Recently, it was also shown that surgical removal of the SCG in mice induces a phenotype resembling dry AMD.¹⁷

In recent years, the field of bioelectronic medicine has emerged with a goal of treating diseases caused by autonomic disbalance.¹⁸ These therapies typically involve electrical stimulation or blocking of autonomic nerves to selectively affect the function of individual organs innervated by those nerves. We hypothesize that chronic electrical modulation of ocular sympathetic activity will slow, stop, or even reverse progression of ocular neovascular diseases by normalizing levels of angiogenic growth factors that regulate blood vessel proliferation. Although prior studies have investigated effects of SCG removal or cervical sympathetic trunk (CST) stimulation on the choroid and retina, the SCG and CST are not practical targets for a clinical neuromodulation therapy. Existing clinical electrodes, which are designed to wrap around or be inserted into nerves, are incapable of interfacing directly with ganglia.¹⁹ Furthermore, the SCG and CST innervate a large number of organs in the head and neck (e.g., salivary, thyroid, parathyroid, and facial sweat glands), and so stimulation of the SCG or CST would likely produce a variety of off-target side effects.^{20,21} Such off-target effects are a leading reason why many bioelectric therapies that have undergone clinical trials fail to achieve commercial success.²² A therapy based on direct neuromodulation of the ICN would potentially overcome these limitations, as it could leverage existing clinical electrode technologies while offering the benefit of ocular specificity. To demonstrate proof of concept of such an approach, we measured the effects of unilateral ICN denervation on changes in choroidal vascularity and angiogenic factors. We also applied acute electrical stimulation of the ICN to investigate the effects of sympathetic activation on choroidal blood flow. To our knowledge, no other studies have investigated the effects of direct ICN modulation on the choroid or retina.

METHODS

Animals

Twenty-seven female Sprague Dawley rats, aged at postnatal day (P) 60 ± 5 days, were used in this study (sex, strain, and age were chosen to be consistent with prior studies).^{8–13} The first group of rats ($n = 20$) underwent unilateral ICN surgical denervation and were euthanized after 6 weeks. Several endpoints were measured in the ipsilateral versus contralateral (control) eye after euthanasia. A second group of rats ($n = 7$) underwent acute electrical stimulation of the ICN while monitoring pupil diameter and choroidal blood flow. All experiments were performed in accordance with the University of Southern California Institutional Animal Care and Use Committee approval and guidelines on animal use and with the ARVO Statement for the Use of Animals in Ophthalmic and Vision Research.

ICN Transection

A technique for rat superior cervical ganglionectomy, previously published by Savastano et al.,²³ was modified in order to selectively transect the ICN while preserving the other SCG

branches (external carotid nerve and cervical sympathetic trunk). Rats were anesthetized with ketamine/xylazine and placed in the supine position in order to expose ventral structures of the neck. A vertical incision was made in the middle of the neck. The incision began 2 cm below the intermandibular region in the presternal region. The skin was retracted and the tissue underneath, including superficial cervical fascia with mandibular glands, was dissected by blunt dissection. Neck muscles were exposed (sternohyoid, omohyoid, sternomastoid, and posterior belly of the digastric muscles), and the carotid triangle was located between the muscles. Within the triangle, the carotid bifurcation was identified and separated into its structures (external and internal carotid arteries; Fig. 1A). The occipital artery and hypoglossal nerve were clearly observed. The SCG was identified below those structures, and the internal and external carotid nerves were exposed (Fig. 1B). The ICN was fully transected 1 mm distal to the SCG, beneath/adjacent to the hypoglossal nerve. Following ICN transection, the skin incision was closed with a nonabsorbable suture (nylon 6-0), and antibiotic ointment was applied.

To verify successful surgery, eyelid and eyeball position were evaluated over the next 3 days.²³ Ptosis of the ipsilateral eyelid was generally observed within 4 to 12 hours after surgery, followed by exophthalmos between 12 and 24 hours. Permanent ptosis ensued around 24 hours after ICN transection (Fig. 1C). Six weeks after surgery, animals were euthanized, and both eyes were removed for further analysis.

Choroidal Vascularity

Choroidal vascularity was measured by histomorphometry in the eyes of five rats. Six weeks after unilateral ICN transection, rats were deeply anesthetized with ketamine/xylazine and perfused transcardially with 20 to 30 mL of cacodylate buffer containing 1% sodium nitrate (to maximally dilate vessels for subsequent histomorphometric analysis^{8,9}). This was followed by perfusion with 200 mL of half-strength Karnovsky's fixative. Eyes were enucleated, hemisected, and posterior portions were immersed in half-strength Karnovsky's fixative overnight. Tissue was embedded in plastic, sectioned at 1- μ m thickness, stained with toluidine blue, and imaged with an Aperio ScanScope slide scanner (Leica Biosystems, Buffalo Grove, IL, USA).

Images were analyzed in Aperio ImageScope software. Measurements were made from an average length of 2 mm of choroid per eye. Choroidal vessels were identified and characterized as arterioles, venules, or capillaries as described previously.^{8,9} All lumina were outlined, and the total surface area occupied by the lumina was extracted. This luminal surface area was divided by the total choroidal surface area in order to calculate the percentage of choroid occupied by blood vessels in each eye. Diameters and counts of each blood vessel type (arterioles, venules, and capillaries) were also determined in each eye. Choroidal thickness was measured at approximately 50- μ m intervals over the length of the tissue and averaged for each eye.

Angiogenic Growth Factor and Inflammatory Marker Levels

The enzyme-linked immunosorbent assay (ELISA) was used to measure protein levels in denervated and control eyes. VEGF and VEGF receptor-2 (VEGFR-2) were measured in the choroid (with albumin as a control), while TNF- α was measured in the retina. Rats ($n = 15$) were euthanized 6 weeks after ICN transection, and eyes were enucleated. Retinas and posterior poles were isolated from each eye. Control and denervated tissues were pooled separately and homogenized in buffer

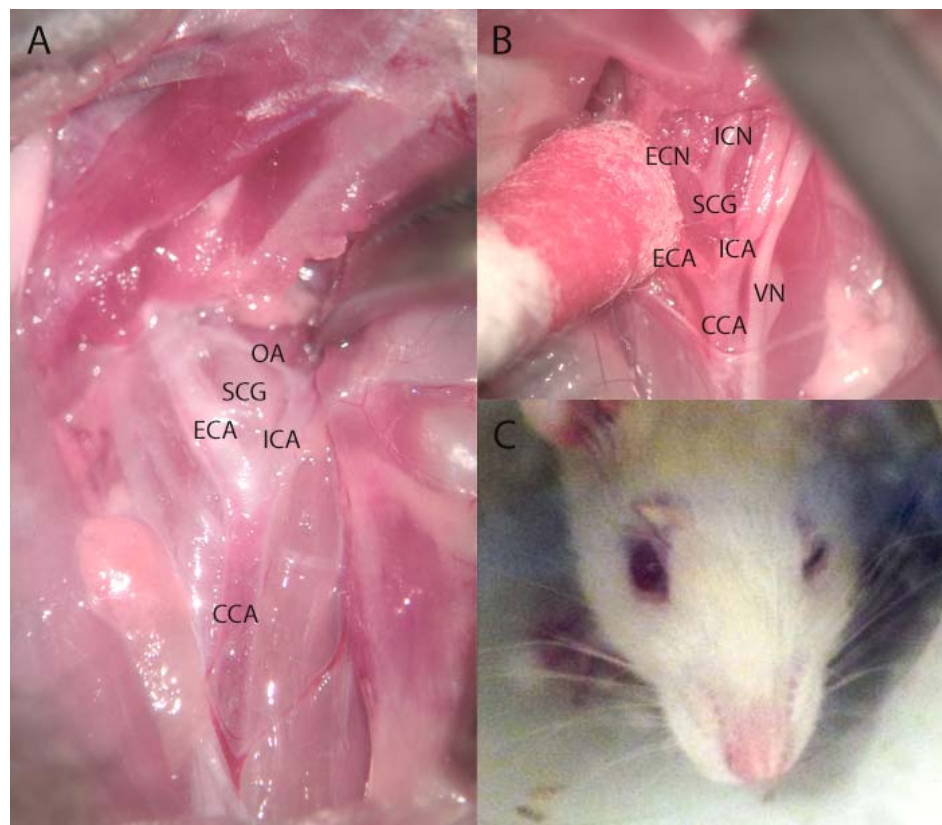


FIGURE 1. ICN transection surgery in rat. (A, B) Photographs of the dissection with anatomic landmarks labeled. (C) Ptosis of the ipsilateral eyelid was observed 24 hours after surgery. OA, occipital artery; ECA, external carotid artery; ICA, internal carotid artery; CCA, common carotid artery; ECN, external carotid nerve; VN, vagus nerve.

containing mixed protease inhibitors for protein extraction. Total protein concentration was determined by a Bio-Rad protein assay (Bio-Rad Laboratories, Hercules, CA, USA). VEGF protein in the posterior poles was assessed with a VEGF ELISA kit (detection range of 3–500 pg/mL; R&D Systems, Minneapolis, MN, USA). VEGFR-2 levels in the posterior poles was assessed with a KDR/VEGFR2/FLK1 ELISA kit (62.5–4000 pg/mL detection range; LifeSpan BioSciences, Seattle, WA, USA). Albumin protein in the posterior poles was assessed with an albumin ELISA kit (1.56–100 ng/mL detection range; Antibodies-Online, Limerick, PA, USA). TNF- α protein in the retinas was assessed with a TNF- α ELISA kit (15–1000 pg/mL detection range; Cell Applications, San Diego, CA, USA). All ELISA assays were performed in triplicate. Protein concentrations were normalized by the total protein.

ICN Stimulation

Seven rats underwent unilateral ICN electrical stimulation while monitoring pupil size and choroidal blood flow. Rats were anesthetized with ketamine/xylazine, and the ICN was exposed as described above (without cutting the nerve). Adipose tissue surrounding the nerve was microdissected away. A bipolar cuff electrode (Micro Cuff Tunnel; CorTec, Freiburg, Germany) with a 200- μ m inner diameter was placed around the ICN and secured with a 6-0 suture knot wrapped around the cuff. Proper placement of the cuff was verified by measuring the electrode impedance with a potentiostat (Gamry Instruments, Warminster, PA, USA). Typical 1-kHz impedance magnitudes ranged from 2 to 10 k Ω .

The ICN was electrically stimulated with charge-balanced biphasic current pulses delivered by an isolated pulse stimulator

(Model 2100; A-M Systems, Sequim, WA, USA). Pulse trains were delivered at a frequency of 7.5, 15, or 30 Hz, and pulse width was set at 100, 200, or 500 μ s/phase. Activation threshold was defined as the minimum current amplitude that caused mydriasis.²⁴ Pupil diameter and choroidal blood flow were monitored before, during, and after acute electrical stimulation. Pupil diameter was measured with calipers under dim light. Blood flow in the anterior and posterior choroid were measured with a laser Doppler monitor (moorVMS-LDF; Moor Instruments, Wilmington, DE, USA) and VP4 blunt needle probe (800- μ m outer diameter). Blood flow recordings from the anterior choroid were made extraocularly by positioning the probe tip in gentle contact with the eye, 2 to 3 mm posterior to the limbus. Posterior choroidal blood flow was measured intraocularly. A superotemporal pars plana incision was made using a 25-G needle, and the blunt needle Doppler probe was introduced into the incision and positioned in the posterior pole (2–3 disc diameters away from optic nerve in the inferior nasal quadrant). The probe was placed in gentle contact with the retina while avoiding retinal vessels. Flux, which is directly proportional to blood flow,²⁵ was recorded with moorVMS-PC software. The time constant was set to 0.5 seconds. Each laser Doppler recording lasted 120 seconds, with electrical stimulation delivered continuously for 30 seconds. Animals were euthanized at the end of the experiment.

RESULTS

Choroidal Vascularity

Figure 2A shows representative toluidine blue-stained sections from a denervated and control choroid. Histomorphometric

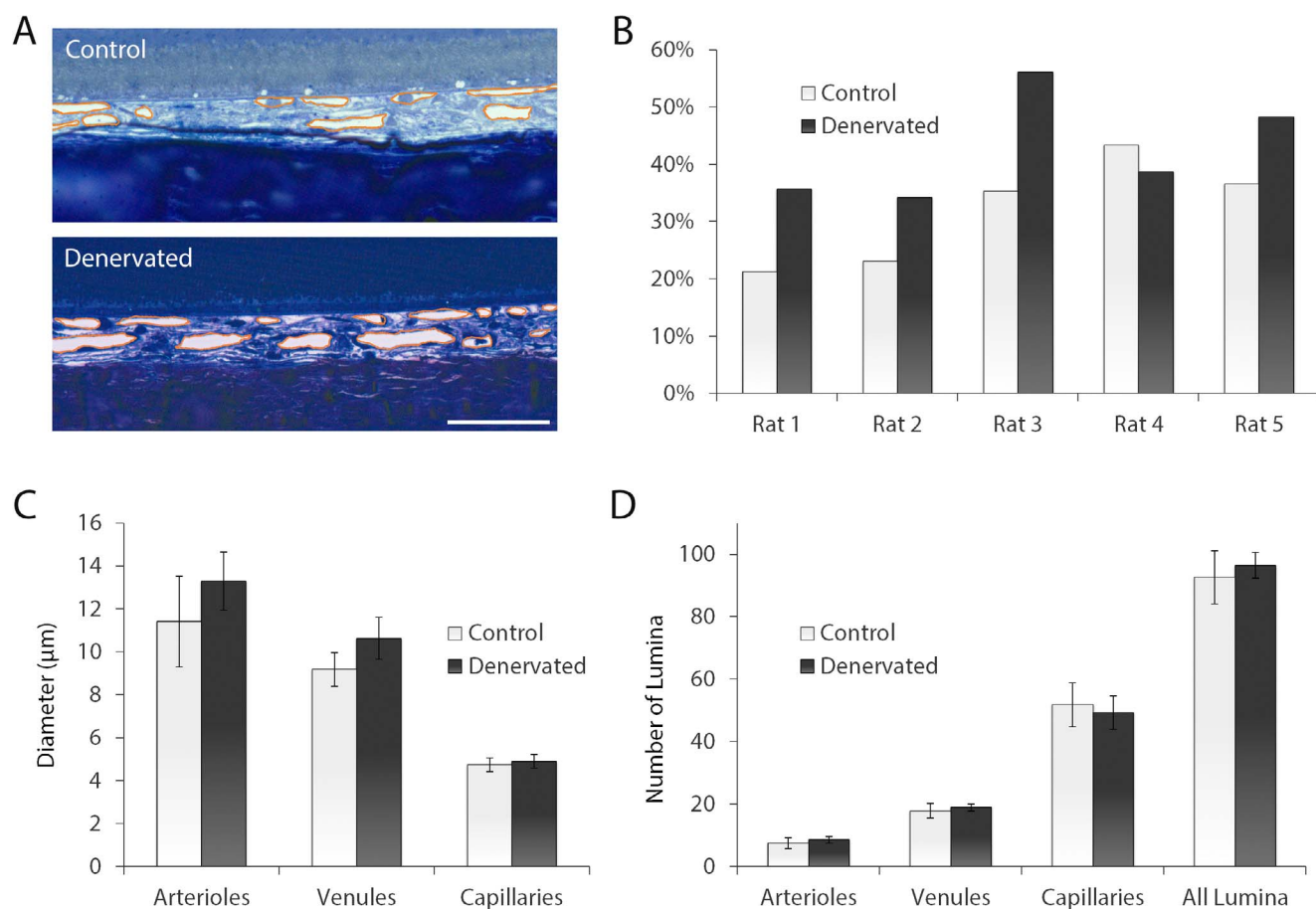


FIGURE 2. Increased choroidal vascularity was observed in denervated eyes. **(A)** Representative images of control and denervated choroids. Blood vessel lumina are outlined in orange. *Scale bar*, 50 μ m. **(B)** Percentage of choroidal surface area occupied by blood vessel lumina in five rats that underwent unilateral ICN transection. Choroidal vascularity increased in four of five animals. **(C, D)** Mean lumen diameter **(C)** and number of lumina per millimeter segment of choroid **(D)** across the five animals. *Error bars* indicate SEM.

analysis revealed that in four of five animals, denervation led to increased choroidal vascularity in sympathectomized eyes (Fig. 2B). Denervated choroids had an average of 42.6% of choroidal surface area occupied by blood vessel lumina, compared with 31.9% in control choroids. This increase in vascularity was caused by a combination of changes in lumen diameter (Fig. 2C) and numbers of lumina (Fig. 2D). Arterioles, venules, and capillaries were larger in denervated choroids than in control choroids, but differences were not statistically significant ($P > 0.05$). Similarly, lumina (except capillaries) were more abundant in denervated choroids but not significantly higher in number than in control choroids ($P > 0.05$). These findings are consistent with those of Steinle et al.,^{8,9} who found that SCG removal in Sprague Dawley rats led to increased choroidal vascularity after 6 weeks. We also measured the choroidal thickness, which was not statistically different between denervated and control eyes (63.1 ± 14.8 and 60.6 ± 17.5 μ m, respectively; $P = 0.81$), unlike Steinle et al.^{8,9} who reported changes in choroidal thickness following sympathectomy.

Angiogenic Growth Factor and Inflammatory Marker Levels

Six weeks following unilateral ICN transection, VEGF, VEGFR-2, and TNF- α protein levels all increased in denervated eyes (Fig. 3). VEGF and VEGFR-2 levels in denervated choroids were 60.5% and 124.4% higher than in contralateral choroids,

respectively. Choroidal albumin levels (measured as a control) were similar in both eyes, indicating that the VEGF and VEGFR-2 changes were not an artifact of increased choroidal vascularity. TNF- α protein in denervated retinas was roughly 3.3-fold more abundant than protein levels in contralateral retinas.

ICN Stimulation

At all pulse durations (100, 200, 500 μ s/phase) and stimulus frequencies (7.5, 15, 30 Hz) tested, electrical stimulation of the ICN at suprathreshold current amplitudes caused mydriasis in the ipsilateral eye while having no apparent effect on the contralateral pupil. When the stimulus was turned on, the pupil gradually dilated until reaching its maximum diameter, tens of seconds later. The time to full dilation was inversely proportional to stimulus amplitude (Fig. 4). Upon cessation of stimulation, the pupil gradually constricted to its original diameter.

ICN stimulation caused reduced choroidal blood flow at all pulse durations and stimulus frequencies, both in the anterior and posterior choroid. At a fixed-pulse duration, the magnitude of the change in blood flow correlated positively with stimulus frequency (Fig. 5A). For a given pulse duration and stimulus frequency, the change in blood flow during suprathreshold stimulation was an all-or-none response (Fig. 5B). Thresholds for affecting choroidal blood flow were higher than pupil dilation thresholds (Figs. 5C, 5D).

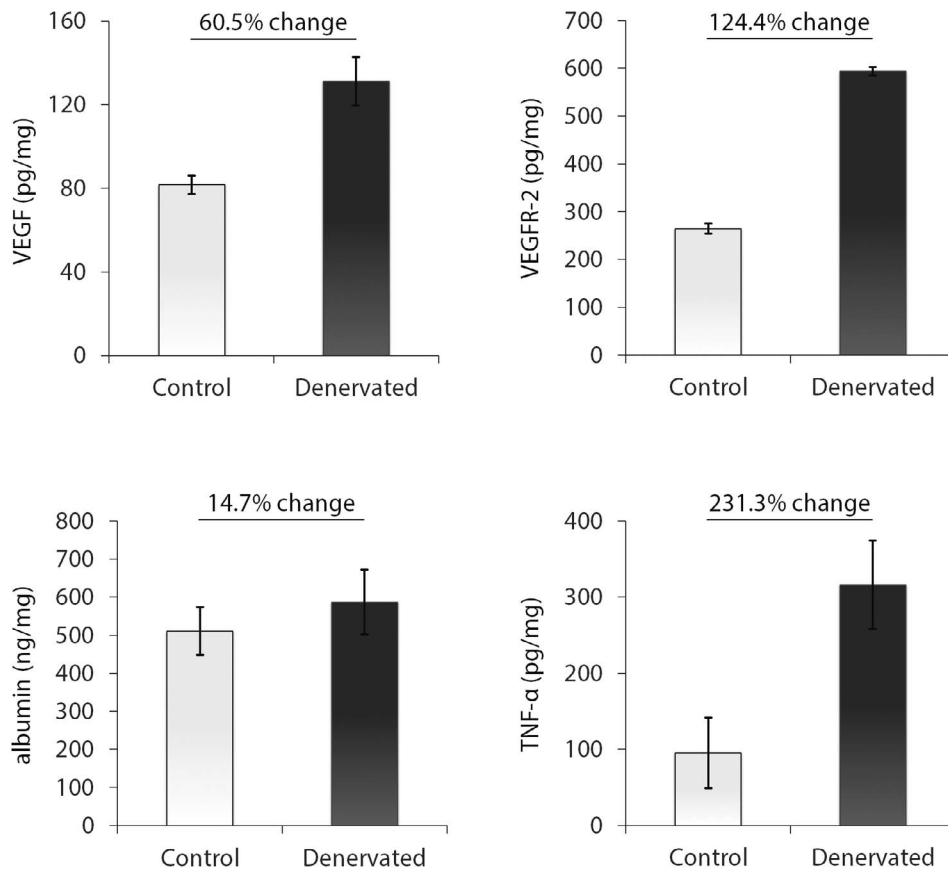


FIGURE 3. Choroidal VEGF, choroidal VEGFR-2, choroidal albumin, and retinal TNF- α protein levels measured by ELISA, 6 weeks after unilateral ICN transection ($n = 15$ rats). Units represent measured protein normalized to total protein. Error bars indicate SD.

DISCUSSION

Collective findings from our study indicate that surgically blocking ocular sympathetic activity through ICN transection has proangiogenic effects. Six weeks after ICN denervation, we observed an increase in choroidal vascularity accompanied by higher levels of proangiogenic factors in the choroid and

retina. Steinle et al.^{8,9} also reported increased choroidal vascularity in Sprague Dawley rats following sympathetic denervation. Although this effect likely arises from remodeling and neovascularization within the choroid, it is possible that the increased choroidal vascularity was indirectly caused by a long-term vasodilation due to a loss of sympathetic tone. In order to avoid the confounding effect of comparing vasodilated choroids in denervated eyes with nonvasodilated choroids in control eyes, animals were perfused with sodium nitrate at the time of euthanasia to cause maximal choroidal vessel dilation.^{8,9} However, it may still be the case that the vessels in denervated choroids were more dilated than those in control choroids, causing the percentage of choroidal surface area occupied by blood vessel lumina to increase. Indeed, we observed larger vessels in denervated versus control eyes (see Fig. 2C), although differences in vessel diameter were not statistically significant.

The increase in choroidal vascularity that we observed may be, in part, due to upregulation of angiogenic growth factors or their receptors (see Fig. 3). Indeed, choroidal VEGF upregulation is observed in AMD patients and has also been reported in rats after SCG removal.^{11,26} However, it should be noted that VEGF upregulation can arise from a number of factors, including inflammation, ischemia, and hypoxia.²⁷ It is possible that sympathetic denervation caused these side effects, leading to an increase in VEGF. A better marker of choroidal remodeling may be VEGF receptor (VEGFR-2) levels. Steinle and Lashbrook¹¹ found that SCG removal caused lower VEGFR-2 protein levels in denervated choroids, despite causing higher VEGF levels. As a result, they concluded that “it is unclear whether VEGF signaling is increased in the choroid following

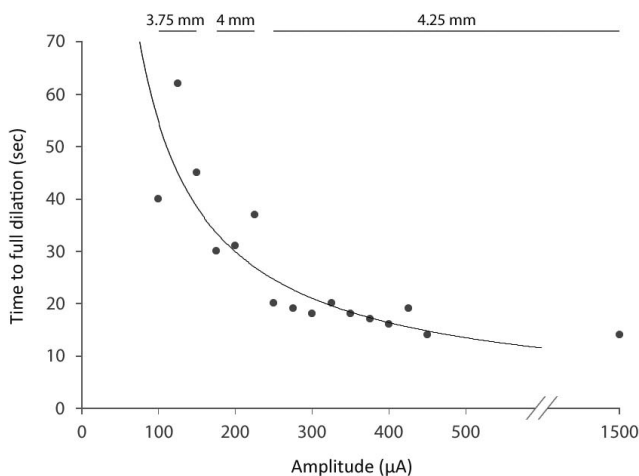


FIGURE 4. Relationship between stimulus amplitude and time to full pupil dilation. Stimulus parameters were 15 Hz, 100 μ s/phase, and 25 to 1500 μ A. Threshold amplitude was measured at 100 μ A. The lines at the top of the chart indicate the pupil diameter when fully dilated, for each stimulus amplitude. Diameter at rest was 3.5 mm.

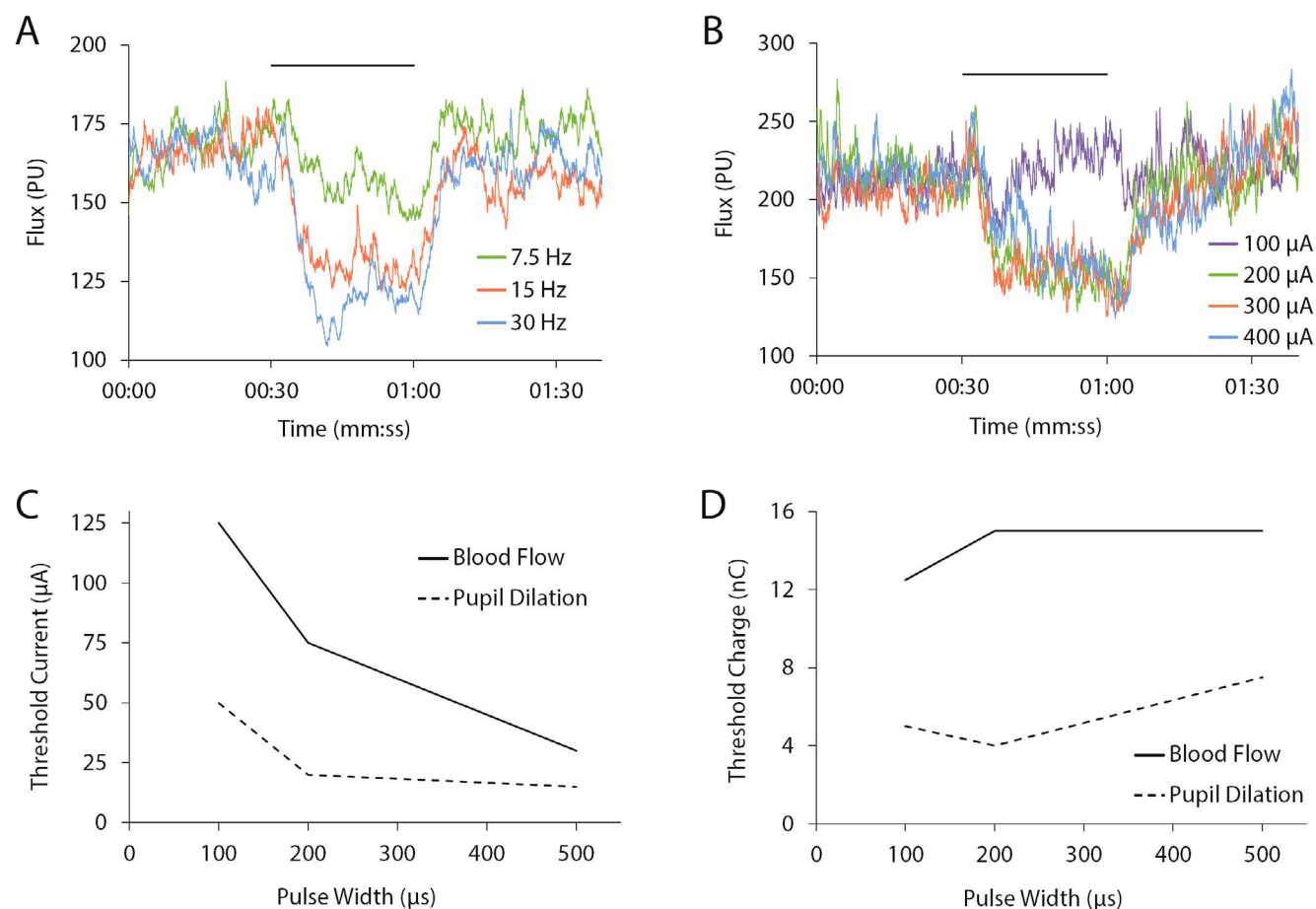


FIGURE 5. Effects of ICN electrical stimulation on choroidal blood flow and pupil size in the ipsilateral eye. **(A)** Laser Doppler flux recordings from anterior choroid during acute ICN electrical stimulation at three frequencies (7.5, 15, and 30 Hz). The stimulus (100 μ s/phase, 150 μ A) was applied between 30 and 60 s (*horizontal line*). Results in the posterior choroid were similar. PU: perfusion units. **(B)** Laser Doppler flux recordings from anterior choroid during acute ICN electrical stimulation at threshold (100 μ A) and suprathreshold amplitudes (200, 300, and 400 μ A). The stimulus (500 μ s/phase, 15 Hz) was applied between 30 and 60 seconds (*horizontal line*). Results in the posterior choroid were similar. **(C, D)** Strength-duration curves for current **(C)** and charge **(D)** showing ICN electrical stimulation thresholds for mydriasis (*dashed line*) and choroidal vasoconstriction (*solid line*).

sympathectomy.” In another study, Wiley et al.¹² found that VEGF and VEGFR-2 levels in the retina were significantly reduced after sympathectomy. Our study showed an opposite effect but in the choroid: choroidal VEGF and VEGFR-2 both increased following ICN transection. Thus, surgically blocking ocular sympathetic activity may have opposing effects on the retina and choroid, at least with regard to angiogenic growth factor levels.

In addition to affecting VEGF and VEGFR-2 levels, ICN transection resulted in elevated amounts of retinal TNF- α protein. This is consistent with findings by Jiang et al.¹⁵ and Panjala et al.,¹⁶ in which β -AR receptor knockout mice exhibited 20% to 30% more retinal TNF- α protein than wild-type mice. TNF- α upregulation is involved in many diseases as oxidative signaling in angiogenesis.²⁸ Upregulation of inflammatory cytokines such as TNF- α is implicated in the pathogenesis of DR.²⁹

As expected, we found that electrical stimulation of the ICN caused a temporary reduction in choroidal blood flow due to vasoconstriction, as well as mydriasis resulting from adrenergic effects on the iris dilator muscle. Other studies in rat have reported decreased uveal blood flow following acute cervical sympathetic trunk stimulation, an effect mediated exclusively by α_1 -ARs.^{30,31} The fact that 100- μ s pulses induced vasoconstriction and mydriasis suggests that these responses are

mediated by A- α fibers, which have chronaxies on the order of 5 to 100 μ s.³²

Targeted therapy based on electrical stimulation of the nervous system, sometimes referred to as bioelectronic medicine, has been under growing investigation in recent years.^{18,33} Our results suggest that modulation of ICN activity could serve as a treatment for ocular neovascular diseases, such as wet AMD and DR. Because transection of the nerve led to increased choroidal vascularity and higher abundance of angiogenic and inflammatory factors, electrical stimulation of the nerve may produce the opposite (i.e., antiangiogenic) effects. ICN electrical stimulation also induces vasoconstriction, which may offer an approach to regulate choroidal blood flow in patients with CNV. While the extent to which our findings will translate to humans is unknown, we chose to conduct this study in rats due to the extensive similarities between rodent and primate ocular sympathetic nerve anatomy and function.^{20,23,34,35} Innervation and neurotransmitter expression patterns in rat and human choroid are similar.³⁴ Additionally, rodents are the most common animal model for investigating ocular therapies that target the β -adrenergic system.⁶ Further experiments should be conducted to determine safety and reliability of ICN stimulation, as well as the translatability of these findings to higher species.

Acknowledgments

The authors thank Danhong Zhu for her help with the ELISA assays.

Supported by a grant from Galvani Bioelectronics to ACW, MSH, and DRH, as well as unrestricted departmental support to the USC Roski Eye Institute from Research to Prevent Blindness.

Disclosure: **J.-C. Martinez-Camarillo**, None; **C.K. Spee**, None; **M. Chen**, None; **A. Rodriguez**, None; **K. Nimmagadda**, None; **G.P. Trujillo-Sanchez**, None; **D.R. Hinton**, Galvani Bioelectronics (F); **A. Giarola**, P; **V. Pikov**, P; **A. Sridhar**, E, P; **M.S. Humayun**, Galvani Bioelectronics (F), P; **A.C. Weitz**, Galvani Bioelectronics (F), P

References

- Campochiaro PA. Ocular neovascularization. *J Mol Med*. 2013; 91:311–321.
- Tong JP, Yao YF. Contribution of VEGF and PEDF to choroidal angiogenesis: a need for balanced expressions. *Clin Biochem*. 2006;39:267–276.
- Virgili G, Parravano M, Evans JR, Gordon I, Lucenteforte E. Anti-vascular endothelial growth factor for diabetic macular oedema: a network meta-analysis. *Cochrane Database Syst Rev*. 2017;6:CD007419.
- Solomon S, Lindsley K, Vedula S, Krzystolik M, Hawkins B. Anti-vascular endothelial growth factor for neovascular age-related macular degeneration. *Cochrane Database Syst Rev*. 2014;8:CD005139.
- McDougal DH, Gamlin PD. Autonomic control of the eye. *Compr Physiol*. 2015;5:439–473.
- Casini G, Dal Monte M, Fornaciari I, Filippi L, Bagnoli P. The β -adrenergic system as a possible new target for pharmacologic treatment of neovascular retinal diseases. *Prog Retin Eye Res*. 2014;42:103–129.
- Smith PG, Reddy H. Reorganization of cranial sympathetic pathways following neonatal ganglionectomy in the rat. *J Comp Neurol*. 1990;301:490–500.
- Steinle JJ, Pierce JD, Clancy RL, Smith PG. Increased ocular blood vessel numbers and sizes following chronic sympathectomy in rat. *Exp Eye Res*. 2002;74:761–768.
- Steinle JJ, Smith PG. Sensory but not parasympathetic nerves are required for ocular vascular remodeling following chronic sympathectomy in rat. *Auton Neurosci Basic Clin*. 2003;109:34–41.
- Steinle JJ, Lindsay NL, Lashbrook BL. Cervical sympathectomy causes photoreceptor-specific cell death in the rat retina. *Auton Neurosci Basic Clin*. 2005;120:46–51.
- Steinle JJ, Lashbrook BL. Cervical sympathectomy regulates expression of key angiogenic factors in the rat choroid. *Exp Eye Res*. 2006;83:16–23.
- Wiley LA, Berkowitz BA, Steinle JJ. Superior cervical ganglionectomy induces changes in growth factor expression in the rat retina. *Invest Ophthalmol Vis Sci*. 2006;47:439–443.
- Lashbrook BL, Steinle JJ. Beta-adrenergic receptor regulation of pigment epithelial-derived factor expression in rat retina. *Aut Neurosci*. 2005;121:33–39.
- Wiley LA, Rupp GR, Steinle JJ. Sympathetic innervation regulates basement membrane thickening and pericyte number in rat retina. *Invest Ophthalmol Vis Sci*. 2005;46:744–748.
- Jiang Y, Zhang Q, Liu L, Tang J, Kern TS, Steinle JJ. β 2-adrenergic receptor knockout mice exhibit a diabetic retinopathy phenotype. *PLoS One*. 2013;8:1–9.
- Panjala SR, Jiang Y, Kern TS, Thomas SA, Steinle JJ. Increased tumor necrosis factor- α , cleaved caspase 3 levels and insulin receptor substrate-1 phosphorylation in the beta(1)-adrenergic receptor knockout mouse. *Mol Vis*. 2011;17:1822–1828.
- Dieguez HH, Romeo HE, González Fleitas MF, et al. Superior cervical gangliectomy induces non-exudative age-related macular degeneration in mice. *DMM Dis Model Mech*. 2018; 11.
- Birmingham K, Gradinaru V, Anikeeva P, et al. Bioelectronic medicines: a research roadmap. *Nat Rev Drug Discov*. 2014; 13:399–400.
- Kim YT, Romero-Ortega MI. Material considerations for peripheral nerve interfacing. *MRS Bull*. 2012;37:573–580.
- Watson C, Vijayan N. The sympathetic innervation of the eyes and face: a clinicoanatomic review. *Clin Anat*. 1995;8:262–272.
- Wang FB, Cheng PM, Chi HC, Kao CK, Liao YH. Axons of passage and inputs to superior cervical ganglion in rat. *Anat Rec*. 2018;301:1906–1916.
- Ludwig K, Ross E, Langhals N, Weber D, Lujan JL, Georgakopoulos D. The autonomic nervous system. In: Dhillon GS, Horch KW. eds. *Neuroprosthetics: Theory and Practice*. Singapore: World Scientific Publishing Company; 2017:12–39.
- Savastano LE, Castro AE, Fitt MR, Rath MF, Romeo HE, Muñoz EM. A standardized surgical technique for rat superior cervical ganglionectomy. *J Neurosci Methods*. 2010;192:22–33.
- Belmonte C, Perez E, Lopez-Briones LG, Gallar J. Chronic stimulation of ocular sympathetic fibers in unanesthetized rabbits. *Invest Ophthalmol Vis Sci*. 1987;28:194–197.
- Kase S, He S, Sonoda S, et al. α B-crystallin regulation of angiogenesis by modulation of VEGF. *Blood*. 2010;115:3398–3406.
- Frank RN. Growth factors in age-related macular degeneration: pathogenic and therapeutic implications. *Ophthalmic Res*. 1997;29:341–353.
- Stefánsson E, Olafsdóttir OB, Einarsson AB, et al. Retinal oximetry discovers novel biomarkers in retinal and brain diseases. *Invest Ophthalmol Vis Sci*. 2017;58: BIO227–BIO233.
- Wang H, Han X, Wittchen ES, Hartnett ME. TNF- α mediates choroidal neovascularization by upregulating VEGF expression in RPE through ROS-dependent beta-catenin activation. *Mol Vis*. 2016;22:116–128.
- Boss JD, Singh PK, Pandya HK, et al. Assessment of neurotrophins and inflammatory mediators in vitreous of patients with diabetic retinopathy. *Invest Ophthalmol Vis Sci*. 2017;58:5594–5603.
- Steinle JJ, Krizan-Agbas D, Smith PG. Regional regulation of choroidal blood flow by autonomic innervation in the rat. *Am J Physiol*. 2000;279:R202–R209.
- Kawarai M, Koss MC. Sympathetic vasoconstriction in the rat anterior choroid is mediated by α 1- adrenoceptors. *Eur J Pharmacol*. 1999;386:227–233.
- Pither CE, Raj PP, Ford DJ. The use of peripheral nerve stimulators for regional anesthesia a review of experimental characteristics, technique, and clinical applications. *Reg Anesth Pain Med*. 1985;10:49–58.
- Mishra S. Electroceuticals in medicine - the brave new future. *Indian Heart J*. 2017;69:685–686.
- Troger J, Kieselbach G, Teuchner B, et al. Peptidergic nerves in the eye, their source and potential pathophysiological relevance. *Brain Res Rev*. 2007;53:39–62.
- Neuhuber W, Schrödl F. Autonomic control of the eye and the iris. *Auton Neurosci Basic Clin*. 2011;165:67–79.